Heliyon

Received:
29 November 2018
Revised:
3 March 2019
Accepted:
18 March 2019

Cite as: Pontip Benjasirimongkol, Suchada Piriyaprasarth, Pornsak Sriamornsak. Design and optimization of resveratrol-loaded porous calcium silicate powders for dissolution and photostability enhancement. Heliyon 5 (2019) e01399.
doi: 10.1016/j.heliyon.2019.e01399

Design and optimization of resveratrol-loaded porous calcium silicate powders for dissolution and photostability enhancement

Pontip Benjasirimongkol [a,b], **Suchada Piriyaprasarth** [a,b], **Pornsak Sriamornsak** [a,b,c,*]

[a] *Department of Pharmaceutical Technology, Faculty of Pharmacy, Silpakorn University, Nakhon Pathom, 73000, Thailand*

[b] *Pharmaceutical Biopolymer Group (PBiG), Faculty of Pharmacy, Silpakorn University, Nakhon Pathom, 73000, Thailand*

[c] *Academy of Science, Royal Society of Thailand, Bangkok, 10300, Thailand*

[*] Corresponding author.
E-mail address: sriamornsak_p@su.ac.th (P. Sriamornsak).

Abstract

In this study, resveratrol (RVT) was loaded onto porous calcium silicate (PCS) powders to improve its dissolution and photostability properties. The effects of RVT/PCS powders that included varying amounts of low-methoxyl pectin (LMP), ethyl acetate (EA) and PCS on drug loading capacity, encapsulation efficiency and drug dissolution at 5-min intervals (Q_5) were investigated using a Box−Behnken design. The experimental results demonstrated that the EA and PCS amounts significantly influenced drug loading capacity. Encapsulation efficiency was affected by EA amount, whereas the amount of PCS had a significant effect on Q_5. Empirical experiments demonstrated the reliability of mathematical models. A design space was established based on the criteria set for maximizing each response of the RVT/PCS powders. An optimized formulation containing 2.6% w/w LMP, 19% w/w EA and 13% w/w PCS prepared within the design space satisfied all criteria. The dissolution and photostability of RVT in the RVT/PCS powders were significantly improved.

https://doi.org/10.1016/j.heliyon.2019.e01399

Further, the bulk density of the PCS powders in RVT/PCS was increased by LMP. The Box−Behnken design used in this study provided an improved understanding of the effects of formulation factors on RVT/PCS powder characteristics as well as the optimization of RVT/PCS powder formulations with the desired properties.

Keywords: Chemical engineering, Pharmaceutical science, Materials science

1. Introduction

In recent decades, the development of delivery systems for drugs and bioactive compounds has increased dramatically in the pharmaceutical industry. Bioactive compounds such as polyphenols and flavonoids possess health benefits owing to their physiological and pharmacological activities [1, 2]. Therefore, bioactive compounds have been studied for the treatment and prevention of diseases, including inflammation, cancer and heart disease [3, 4, 5].

Resveratrol (RVT) is one of the most interesting polyphenols because it possesses various potential advantages to human health such as in the treatment of diabetes, cancer, aging and cardiovascular disease [6]. However, from the viewpoint of product development, RVT has some disadvantages such as poor water solubility and photo-sensitivity [7, 8]. Various dosage forms have been studied to assess their potential to enhance the dissolution and stability of RVT such as within emulsions [9], nanoparticles [10], liposomes [11] and complexes using cyclodextrin [12]. However, some degradation of RVT after UV irradiation has been observed in previous studies [13, 14, 15]. Therefore, an appropriate drug delivery system is required to improve the dissolution properties of RVT and protect it from light degradation, such as encapsulation.

Various porous materials, e.g., porous silicon dioxide, porous calcium silicate (PCS), have been studied as adsorbent carriers for drug delivery systems. PCS is one option for enabling improvements in the dissolution properties of drugs possessing poor water solubility [16, 17]. Previous study revealed that spontaneous emulsifying powders using PCS provided a faster dissolution of drug compared to other porous materials, i.e., fumed silica and porous silicon dioxide [18]. The high number of pores in PCS provides a large surface area and pore volume, leading to a high adsorption capacity. Nevertheless, PCS has certain disadvantages for drug delivery systems. The intrinsically low density of PCS retards pharmaceutical development from the viewpoint of the manufacturing process [19]. Density differences between the components during formulation may cause non-homogeneous mixing and segregation during processing. A previous study used a wet granulation technique to increase the bulk density of PCS powders during formulation [20]. In our study, we implemented another technique to increase the bulk density of PCS.

https://doi.org/10.1016/j.heliyon.2019.e01399

To obtain RVT/PCS powders with the desired quality, e.g. having a high drug loading capacity, encapsulation efficiency or drug dissolution, the relationship between formulation factors and product quality must be clearly understood. Design of experiment (DoE) considerations can provide an extensive understanding of the effects of independent factors on responses (both efficiently and economically) owing to the small number of experiments required [21]. Previous studies have applied the DoE approach to experiments on porous materials [22, 23]. The Box−Behnken design is one type of DoE and is a commonly applied response surface methodology (RSM) for optimization studies of formulations or processes. Compared with RSM designs containing the same number of independent factors, the Box−Behnken design can be performed with fewer experimental runs and provides sufficient information for an optimization study. The relationship between the independent factors and responses can be described using design space [24]. The design space can help determine the ranges of independent factors within which consistent responses can be achieved. As such, the relevant quality attributes of a product can be achieved when production takes place within the design space region.

In the present work, we developed RVT-loaded PCS powder formulations using an emulsion system and solvent evaporation. PCS powders were used to improve the dissolution properties of RVT. The effects of formulation factors on the characteristics of RVT-loaded PCS powders, including drug loading capacity, encapsulation efficiency and drug dissolution, were determined using the Box−Behnken design. The RVT-loaded PCS powder formulations were optimized to be produced with specific properties within a developed design space. Based on the optimization study, the optimal range for each formulation factor was revealed.

2. Materials and methods

2.1. Materials

RVT was obtained from Sami Lab Ltd. (Tumkur, India). PCS (Florite® RE) was provided by Eisai R&D Management Co., Ltd. (Kobe, Japan). Low-methoxyl pectin (LMP; molecular weight = 70 kDa, degree of esterification = 38%) was provided by Herbstreith & Fox Corporate Group (Neuenbürg, Germany). Ethyl acetate (EA) was purchased from RCI Labscan Ltd. (Bangkok, Thailand). Distilled water was used as the aqueous phase in preparations. Other pharmaceutical-grade chemicals were used as received.

2.2. Experimental design

In the present study, a Box−Behnken design was used to optimize RVT-loaded PCS powder formulations (RVT/PCS powders) and investigate the effect of selected independent factors on the responses. The independent factors with the design levels

https://doi.org/10.1016/j.heliyon.2019.e01399

and responses are shown in Table 1. The levels of each independent factor were selected based on results obtained from preliminary experiments. Design-Experts® version 8.0.7.1 (Stat-Ease Inc., Minneapolis, USA) was utilized to design the experiments, which created 15 experiments and two center points. All the experiments from standard order (S1−17) were randomized and performed as per the run order to avoid any bias. Partial model sum of squares and lack-of-fit tests were performed for linear, two-factor interaction and quadratic models for each response. A significant *p*-value from the partial model sum of squares analysis and a non-significant lack-of-fit *p*-value were used as criteria to select the model. The obtained model was simplified using backward elimination to remove unimportant predictors in the equation and improve model adequacy. The model of each response was verified from the results of additional experiments and the deviation from the predicted value was determined based on the root mean square error (RMSE) as shown in Eq. (1).

$$\mathrm{RMSE} = \sqrt{\frac{\sum_{i=1}^{n}\left(\hat{y}_i - y_i\right)^2}{n}} \tag{1}$$

where, $(\hat{y}_i - y_i)$ is the residual or difference between the predicted value $(\hat{y}_i)$ and observed value (y_i) for $i = 1$ to n, where n is number of the experiment [25].

The design space was developed according to the criteria of each response and the desirability function. An optimized batch was produced from the optimal value within the obtained design space. The residual and percent error of results obtained from the optimized and predicted values were calculated as shown in Eqs. (2) and (3), respectively.

$$\mathrm{Residual} = \hat{y}_i - y_i, \tag{2}$$

Table 1. Independent factors in Box−Behnken design and responses of resveratrol (RVT)-loaded porous calcium silicate (PCS) powders.

Independent factors	Low level	Medium level	High level
X_1: LMP amount (% w/w)	2	2.5	3
X_2: EA amount (% w/w)	10	15	20
X_3: PCS amount (% w/w)	10	15	20
Responses			
Y_1: Drug loading capacity (%)			
Y_2: Encapsulation efficiency (%)			
Y_3: Drug dissolution at 5-min intervals (Q_5; %)			

https://doi.org/10.1016/j.heliyon.2019.e01399

$$\text{Error}\ (\%) = \left|\frac{\hat{y}_i - y_i}{y_i}\right| \times 100 \quad (3)$$

2.3. Preparation of RVT/PCS powders

Oil-in-water emulsions containing RVT were prepared by a homogenization process. The LMP amounts (2−3% w/w) and EA amounts (5−10% w/w) were varied in the RVT emulsions. The dispersed phase was EA, containing RVT at a concentration of 17 mg/mL. LMP dissolved in distilled water was used as the aqueous phase. Homogenization was performed using a homogenizer (model Polytron PT 10-35 GT, Kinematica AG, Luzern, Switzerland) at a speed of 18,000 rpm for 10 min. The RVT emulsion was gradually added and adsorbed onto PCS powders (10−20% w/w) using a mortar and pestle for 3 min to prepared granulated wet mass. The RVT emulsion-loaded PCS powders were dried overnight at 40 °C in a vacuum oven (model Vacucell 55, MMM Medcenter Einrichtungen GmbH, Munich, Germany) to yield RVT/PCS powders. The EA containing RVT was also loaded onto PCS powders, as a control formulation, under the same conditions.

2.4. Evaluation of drug loading capacity and encapsulation efficiency

RVT contents were measured using high performance liquid chromatography (HPLC; model Jasco PU-2089 plus quaternary gradient inert pump and a Jasco UV-2070 plus multi wavelength UV-Vis detector, Jasco, Tokyo, Japan). The RVT/PCS powders were dissolved in a mobile phase containing a mixture of methanol, water and glacial acetic acid at a volume ratio of 55:44:1. The sample solutions were filtered through a 0.45-μm nylon filter before being applied to a reversed phase C18 column (25 cm × 4.60 mm; particle size = 5 μm; Phenomenex Inc., California, USA). The flow rate and injection volume were 1 mL/min and 20 μL, respectively. The RVT concentration was measured by UV absorption at 307 nm. The retention time of RVT was approximately 5 min. Linearity was performed using a RVT standard within a concentration range of 0.01−50 μg/mL. The drug loading capacity in the RVT/PCS powders and the encapsulation efficiency of the RVT/PCS powders were calculated from Eqs. (4) and (5), respectively [26].

$$\text{Drug loading capacity}\ (\%) = \frac{\text{Total RVT amount}\ (\text{mg}) \times 100}{\text{Amount of RVT/PCS powders}\ (\text{mg})}, \quad (4)$$

$$\text{Encapsulation efficiency}\ (\%) = \frac{\text{Total RVT amount}\ (\text{mg}) \times 100}{\text{Initial amount of RVT}\ (\text{mg})} \quad (5)$$

https://doi.org/10.1016/j.heliyon.2019.e01399

2.5. Determination of particle morphology

The morphology of the RVT/PCS powders was evaluated using a scanning electron microscope (SEM; model LEO 1450 VP, LEO Electron Microscopy Ltd., Cambridge, UK). The samples were fixed on the stub and then coated with a thin gold layer before determination. An accelerating voltage of 10.0 kV and a working distance of 11 mm were applied to obtain the images.

2.6. Porosimetry measurement

Surface area, pore volume and pore size of intact PCS and RVT/PCS powders were evaluated using a surface area and pore size analyzer (model Nova 2000e, Quantachrome, USA). Samples were degassed for 2 hours at 100 °C using a vacuum to remove residual water. Adsorption and desorption isotherms were collected at 77 K. Surface area, pore volume and pore size were calculated using the Beret–Joyner–Halenda (BJH) method.

2.7. Viscosity measurement

Selected samples were evaluated for viscosity by a dynamic shear rheometer (model Kinexus, Malvern Panalytical Ltd., Malvern, UK) endowed with a cone–plate geometry with a diameter of 50 mm. The shear rate profile was 0.1–100 s^{-1}. Measurement of each sample was performed in triplicate at 25 °C.

2.8. Powder X-ray diffraction (PXRD) measurement

The PXRD measurement was conducted using a powder X-ray diffractometer (model Miniflex II, Rigaku Corp., Tokyo, Japan) under the following conditions: 30kV, 15 mA and angle speed of 4°/min over the range of 5o–45° 2θ using Cu Kα radiation wavelength of 1.5406 Å.

2.9. Differential scanning calorimetry (DSC) measurement

The DSC measurement was carried out using a differential scanning calorimeter (model Sapphire, Perkin Elmer Inc., MA, USA). Approximately 5 mg of sample was placed in a crimped aluminium pan. Then, dry nitrogen was used as insert gas at a flow rate of 50 mL/min. The measurements were performed by heating from 30 to 300 °C at a heating rate of 10 °C/min.

2.10. *In vitro* drug dissolution study

The *in vitro* drug dissolution of RVT/PCS powders was evaluated using a USP dissolution apparatus 4 or flow-through cell apparatus (model CE7 smart with a

https://doi.org/10.1016/j.heliyon.2019.e01399

CY7 piston pump, Sotax AG, Aesch, Switzerland). A 5-mm ruby bead was placed in the cone of the flow-through cell; the cone had a diameter of 12 mm and was filled with 1-mm glass beads. The closed system was controlled at 37 ± 0.1 °C. RVT in the RVT/PCS powders (equivalent to 0.2 mg) was used to ensure the sink condition in a dissolution medium of acetate buffer (pH 4.5). The RVT/PCS powders were placed in the sample cell. Then, 100 mL of the dissolution medium was flowed circularly at a flow rate of 8 mL/min. At specified time intervals, 4 mL samples were withdrawn and replaced with fresh medium. The samples were centrifuged at a speed of 15,000 rpm for 30 min, and the supernatant was analyzed using a T60 UV-Vis spectrophotometer (PG instrument Ltd., Leicestershire, UK) at 307 nm. The drug dissolution study was performed in triplicate.

2.11. Bulk density determination

The bulk density of intact PCS, optimized RVT/PCS powders and PCS containing the same amount of RVT as the optimized formulation were measured using a graduated cylinder. A 2-g sample was poured into a 50-mL graduated cylinder and the volume observed was used in the calculation of bulk density as shown in Eq. (6).

$$\text{Bulk density } (\text{g/cm}^3) = \frac{\text{Sample weight (g)}}{\text{Sample volume (cm3)}} \quad (6)$$

2.12. Photostability of RVT in RVT/PCS powders

RVT/PCS powders were spread uniformly on a glass petri dish to allow uniform irradiation. A sample was placed inside a UV chamber to protect samples from extraneous light and positioned 10 cm below a Spectroline UV lamp (model ENF-260/FE, Spectronics Corporation, New York, USA) at 25 ± 5 °C and 60 ± 5% relative humidity. The sample was exposed to the UV irradiation at 356 nm and withdrawn at 30 min and 60 min before drug content analysis. Each sample was analyzed in triplicate by HPLC method and the remaining *trans*-RVT content after UV exposure was recorded. RVT emulsions was exposed to UV light for the comparison.

3. Results and discussion

Seventeen RVT/PCS powder formulations were prepared using the Box−Behnken design. The formulation factors were LMP amount (X_1), EA amount (X_2) and PCS amount (X_3). The responses of the RVT/PCS powders were drug loading capacity (Y_1), encapsulation efficiency (Y_2) and Q_5 (Y_3). The formulations of the RVT/PCS powders and the response results are shown in Table 2.

https://doi.org/10.1016/j.heliyon.2019.e01399

Table 2. Box−Behnken experimental design layout and response results for RVT/PCS powders.

Standard order (S)	Run order	Independent factors			Responses		
		LMP amount (% w/w)	EA amount (% w/w)	PCS amount (% w/w)	Drug loading capacity (%)	Encapsulation efficiency (%)	Q_5 (%)
1	6	2	10	15	0.51 ± 0.07	60.34 ± 0.41	53.94 ± 5.72
2	5	3	10	15	0.50 ± 0.05	66.49 ± 6.31	53.51 ± 4.27
3	12	2	20	15	1.39 ± 0.01	89.65 ± 0.95	47.07 ± 4.49
4	8	3	20	15	1.38 ± 0.15	98.80 ± 0.81	46.13 ± 3.57
5	11	2	15	10	1.55 ± 0.07	90.99 ± 0.31	21.48 ± 2.97
6	14	3	15	10	1.43 ± 0.03	88.64 ± 1.89	37.59 ± 4.48
7	3	2	15	20	0.78 ± 0.05	91.22 ± 5.36	44.54 ± 5.82
8	9	3	15	20	0.72 ± 0.05	84.71 ± 4.30	59.16 ± 2.64
9	2	2.5	10	10	0.86 ± 0.01	75.82 ± 0.63	30.38 ± 1.81
10	16	2.5	20	10	2.16 ± 0.04	97.61 ± 1.73	32.75 ± 1.31
11	7	2.5	10	20	0.32 ± 0.05	62.20 ± 1.58	54.86 ± 3.14
12	13	2.5	20	20	1.03 ± 0.07	88.76 ± 1.93	63.54 ± 5.12
13	15	2.5	15	15	0.83 ± 0.01	72.82 ± 0.96	56.24 ± 6.43
14	1	2.5	15	15	0.89 ± 0.06	81.50 ± 2.43	47.16 ± 5.59
15	4	2.5	15	15	0.99 ± 0.07	86.72 ± 5.73	56.54 ± 1.96
16	17	2.5	15	15	0.98 ± 0.08	81.89 ± 3.12	47.54 ± 3.20
17	10	2.5	15	15	0.87 ± 0.09	71.54 ± 2.20	45.57 ± 6.63

3.1. Drug loading capacity of RVT/PCS powders

A high amount of drug loaded into a powder is a desirable formulation property. The effect of each independent factor on the drug loading capacity of the RVT/PCS powders was investigated using statistical analysis. The drug loading capacity of RVT/PCS powders varied from 0.32% ± 0.05%−2.16% ± 0.04%, as summarized in Table 2. The significance and the effect of each independent factor were determined using ANOVA. A mathematical model used to describe the relationship between the various factors and drug loading capacity of the RVT/PCS powders is shown in Eq. (7).

$$\text{Drug loading capacity (\%)}: Y_1 = +1.01 + 0.47X_2 - 0.39X_3 - 0.15X_2X_3 \quad (7)$$

From the ANOVA results (Table 3), the mathematical model for predicting drug loading capacity of RVT/PCS powders was significant (p-value < 0.0001) and lack of fit was not significant. The model predicting drug loading capacity showed a high r^2 value of 0.9447, which demonstrates the reliability of the model. ANOVA showed that effect of EA amount (X_2), PCS amount (X_3) and the interaction between

https://doi.org/10.1016/j.heliyon.2019.e01399

Table 3. ANOVA results for model predicting drug loading capacity (Y_1), encapsulation efficiency (Y_2) and Q_5 (Y_3).

Source	Sum of Squares	Degree of freedom	Mean square	F value	*p*-value, Prob > F
For Y_1 (%)					
Model	3.1	3	1.03	74.09	<0.0001
X_2	1.78	1	1.78	127.31	<0.0001
X_3	1.24	1	1.24	88.64	<0.0001
X_2X_3	0.088	1	0.088	6.32	0.0259
Residual	0.18	13	0.014		
Lack of fit	0.16	9	0.018	3.98	0.0981
Pure error	0.018	4	4.55E-03		
Cor Total	3.28	16			
Other statistics: $r^2 = 0.9447$, adjusted $r^2 = 0.9320$, predicted $r^2 = 0.8900$, RMSE = 0.012					
For Y_2 (%)					
Model	1800.35	4	450.09	16.99	0.0001
X_2	1511.64	1	1511.64	57.06	<0.0001
X_3	85.74	1	85.74	3.24	0.0995
X_2^2	94.18	1	94.18	3.56	0.086
X_3^2	108.78	1	108.78	4.11	0.0677
Residual	291.4	11	26.49		
Lack of fit	191.04	8	23.88	0.71	0.6884
Pure error	100.36	3	33.45		
Cor Total	2091.75	15			
Other statistics: $r^2 = 0.8607$, adjusted $r^2 = 0.8100$, predicted $r^2 = 0.7129$, RMSE = 5.15					
For Y_3 (%)					
Model	1585.53	3	528.51	17.49	<0.0001
X_1	107.75	1	107.75	3.57	0.0815
X_3	1247.5	1	1247.5	41.28	<0.0001
X_3^2	230.27	1	230.27	7.62	0.0162
Residual	392.85	13	30.22		
Lack of fit	279.25	9	31.03	1.09	0.5046
Pure error	113.59	4	28.4		
Cor Total	1978.37	16			
Other statistics: $r^2 = 0.8014$, adjusted $r^2 = 0.7556$, predicted $r^2 = 0.6430$, RMSE = 5.50					

Note: $p < 0.05$ is considered as significant; Cor total = corrected total sum of square; RMSE = root mean square error.

EA amount and PCS amount (X_2X_3) were significant. The EA amount showed a positive association whereas PCS amount and interaction between EA amount and PCS amount showed negative associations with drug loading capacity of the RVT/PCS powders. The drug loading capacity increased with increasing EA amount and decreasing PCS amount. The effect of each significant factor was illustrated using a contour plot. From the contour plot (Fig. 1), an increase in EA and a reduction in PCS amount evidently enhanced the drug loading capacity of the RVT/PCS

https://doi.org/10.1016/j.heliyon.2019.e01399

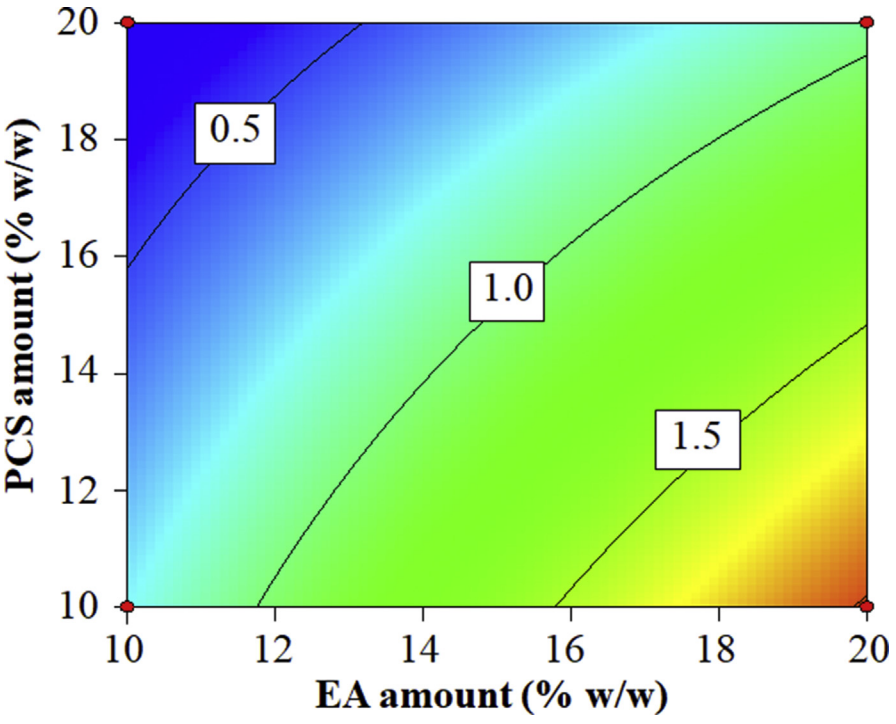

Fig. 1. Contour plot showing effect of porous calcium silicate (PCS) amount and ethyl acetate (EA) amount on drug loading capacity of resveratrol (RVT)/PCS powders.

powders. The content of RVT depended on the concentration of the dispersed phase (EA containing RVT) in the emulsion. High concentration of dispersed phase in the formulation led to an increase in the RVT adsorbed on the RVT/PCS powders. On the contrary, PCS amount showed a negative influence on drug loading capacity. The formulation containing a high content of PCS had a low amount of emulsion in the formulation, which subsequently led to a lower loading of RVT in the RVT/PCS powders. A previous study reported that varying the volume of the solvent in the dried adsorbed powder formulation induces differences in drug adsorption onto porous powders [27]. In a similar manner, the drug loading capacity of RVT/PCS powders was dependent on the EA amount and PCS amount in the formulation.

Fig. 2 shows the surface morphology of intact PCS and RVT/PCS powders (batch S10). Intact PCS exhibited petal-like flakes on its surface. In comparison, the surface of the RVT/PCS powder, which contained the highest amount of RVT among all the RVT/PCS powders, showed the formation of stacks on the PCS surface (Fig. 2-b2). The porosimetry results showed that intact PCS has a surface area of 83.82 m^2/g, pore radius of 16.93 Å and pore volume of 0.46 cc/g, whereas the surface area, pore radius and pore volume of the RVT/PCS powders were 63.29 m^2/g, 16.23 Å and 0.34 cc/g, respectively. The adsorption and desorption isotherms of intact PCS and RVT/PCS powders revealed mesopores type of these samples (Fig. 3). The decrease in pore volume in the RVT/PCS powder, as compared with the intact

https://doi.org/10.1016/j.heliyon.2019.e01399

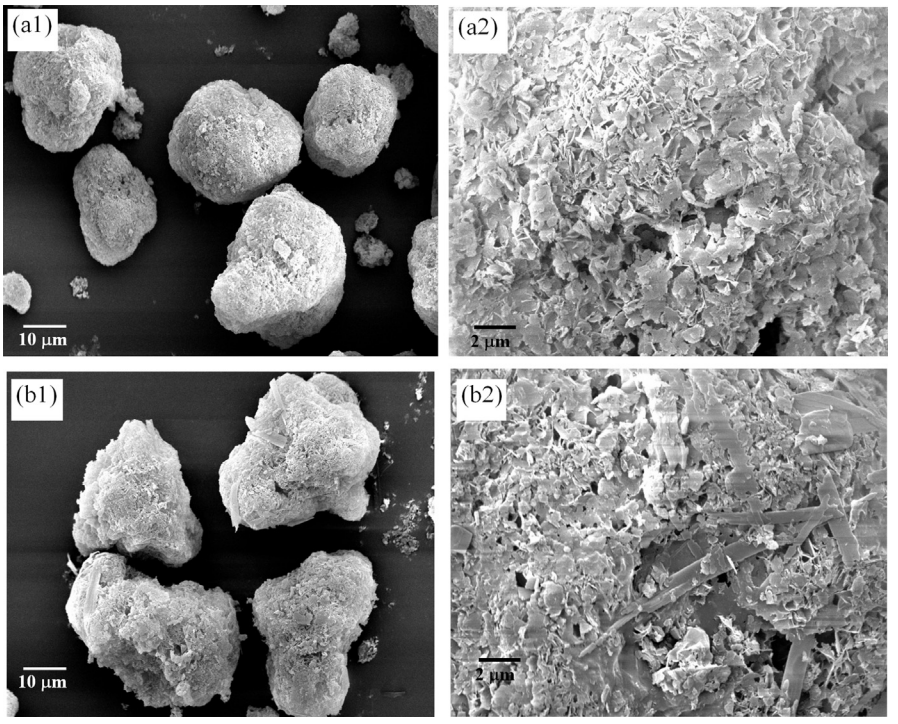

Fig. 2. Scanning electron microscope images of intact PCS at magnifications of (a1) 1000× and (a2) 5000× and RVT/PCS powders standard order (S) 10 at magnifications of (b1) 1000× and (b2) 5000×.

PCS, was due to the adsorption of RVT and LMP onto the PCS powder. The decrease in surface area was due to a blocking of pores in the presence of the drug [28]. In the case of the RVT/PCS powder, the reduction of both pore volume and surface area could be due to the adsorption of both RVT and LMP on the PCS surface. However, the pore volume of RVT/PCS powders was not markedly decreased because the high amount of water and ethyl acetate in the RVT emulsions adsorbed before drying. The pore size of intact PCS and the RVT/PCS powders was similar, indicating that the emulsion did not affect the pore size of PCS.

3.2. Encapsulation efficiency of RVT/PCS powders

It was also necessary to study the factors affecting the encapsulation efficiency of RVT/PCS powders. A high encapsulation efficiency could show the effectiveness of the loading method of the RVT/PCS powders. The encapsulation efficiency of the RVT/PCS powders ranged from 60.34% ± 0.41%−98.80% ± 0.81% (Table 2). A mathematical model used to describe the relationship between the various factors and the encapsulation efficiency of the RVT/PCS powders is shown in Eq. (8).

$$\text{Encapsulation efficiency } (\%): Y_2 = + 82.2 + 13.75X_2 - 3.27X_3 - 4.85X_2^2 + 5.21X_3^2 \quad (8)$$

https://doi.org/10.1016/j.heliyon.2019.e01399

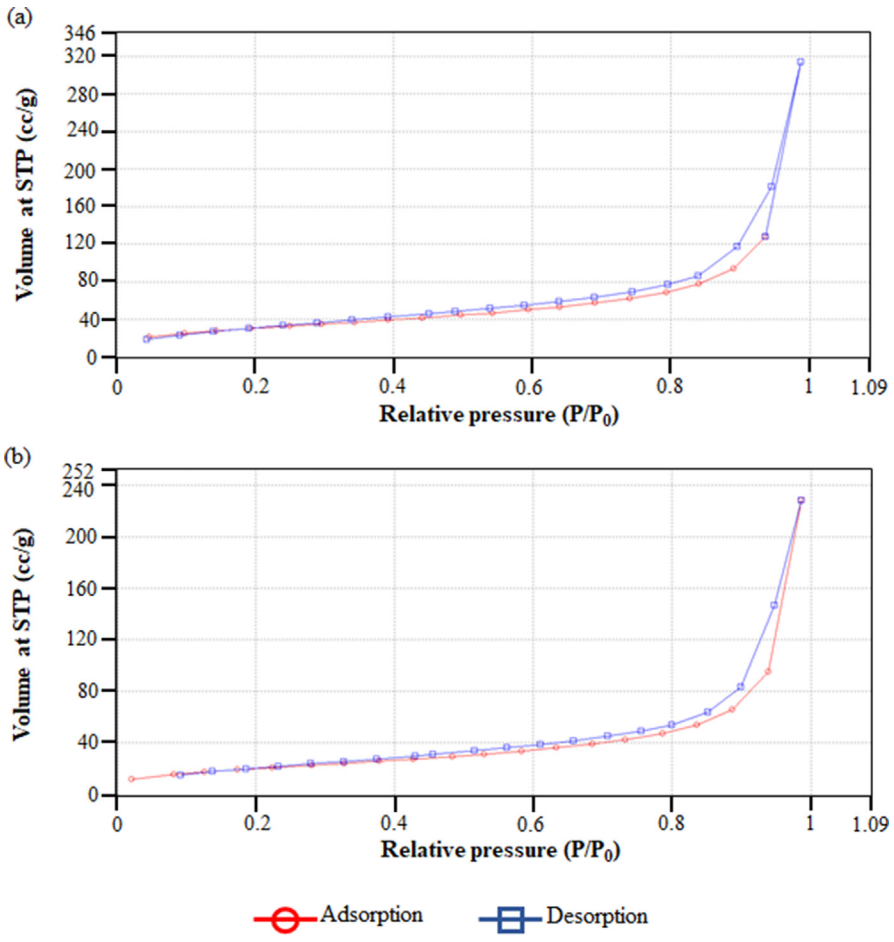

Fig. 3. Adsorption and desorption isotherms of (a) intact PCS and (b) RVT/PCS powders.

From the ANOVA results (Table 3), the mathematical model for predicting the encapsulation efficiency of the RVT/PCS powders was significant ($p < 0.05$) and lack of fit was not significant. The model showed a high r^2 value of 0.8607. ANOVA showed that effect of EA amount (X_2) was the most significant. EA amount showed a positive association with the encapsulation efficiency of the RVT/PCS powders. From the contour plot (Fig. 4), the high amount of EA in the emulsion led a relatively high encapsulation efficiency of the RVT/PCS powders, as compared with the formulation containing lower EA amount. EA containing dissolved RVT may have been adsorbed by the surface of the PCS powders. The increase in encapsulation efficiency of the formulation containing a high amount of EA may have been due to the viscosity difference between EA and the water phase in the emulsion. The viscosity of EA was 1.08 ± 0.03 mPa·S at a shear rate of 3.13 S^{-1} at 25 °C, whereas that of water was significantly higher, 2.50 ± 0.09 mPa·S under the same conditions: such differences have been reported previously [29]. In addition, the high amount of EA facilitated the adsorption of EA onto PCS powders owing to the increase in pressure gradient. The pressure gradient replaces capillary action

https://doi.org/10.1016/j.heliyon.2019.e01399

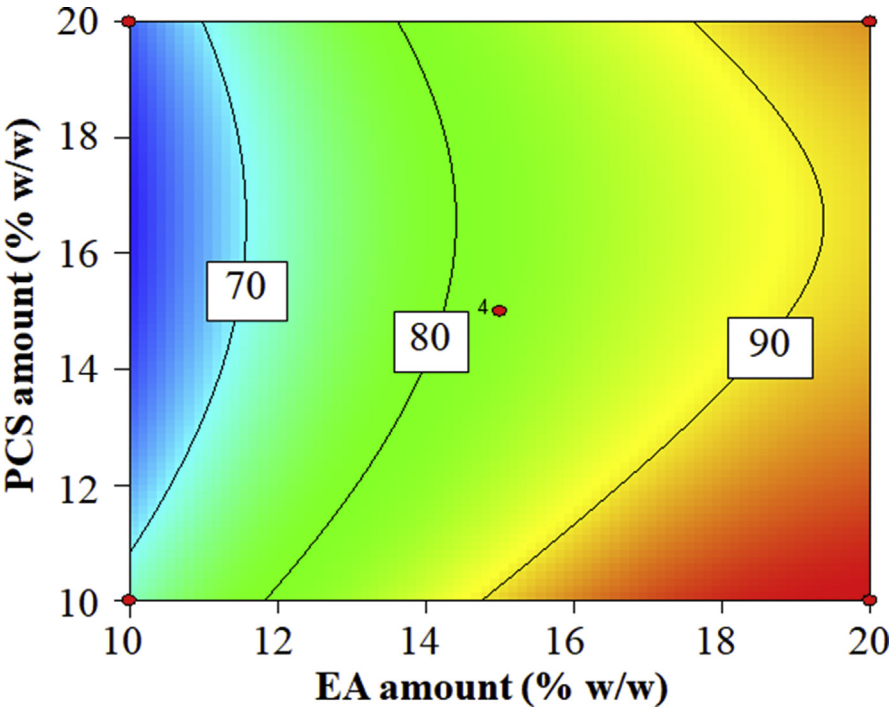

Fig. 4. Contour plot showing the effect of PCS amount and EA amount on encapsulation efficiency of RVT/PCS powders.

when an adsorbent is completely submerged in an adsorbate [30]. An increase in solvent volume may assist the migration of solvent-containing drugs deep inside the pores of an adsorbent [27]. Therefore, the high amount of EA in the RVT/PCS powders may have induced the higher encapsulation efficiency, as compared with that containing the lower amount of EA.

3.3. *In vitro* drug dissolution

Fig. 5a shows dissolution profiles of intact RVT and RVT/PCS powders (batches S9 and S11). The dissolution of the intact RVT was ~10% at 120 min, indicating the intrinsically poor water solubility of RVT. In contrast, both RVT/PCS powders (batch S9 and S11) showed relatively high drug dissolution. The dissolution properties of RVT were also improved in other formulations, as shown in Table 2. This suggests that the RVT/PCS powders significantly improved the dissolution properties of RVT. Ali et al. suggested that the dissolution of crystalline drugs loaded into porous powders is improved owing to a reduction in crystalline size, resulting in an increase in the surface area of the crystalline drug [31]. Therefore, in this study, the improved dissolution of RVT when loaded into porous powders may have been due to the reduction of crystalline RVT size. A previous study reported that the volume of an RVT single crystal was 1075.5 $Å^3$ [32]. From our porosimetry results, the pore radius of PCS was 16.23 Å and the volume was 4275.2 $Å^3$. The pore size of PCS was

https://doi.org/10.1016/j.heliyon.2019.e01399

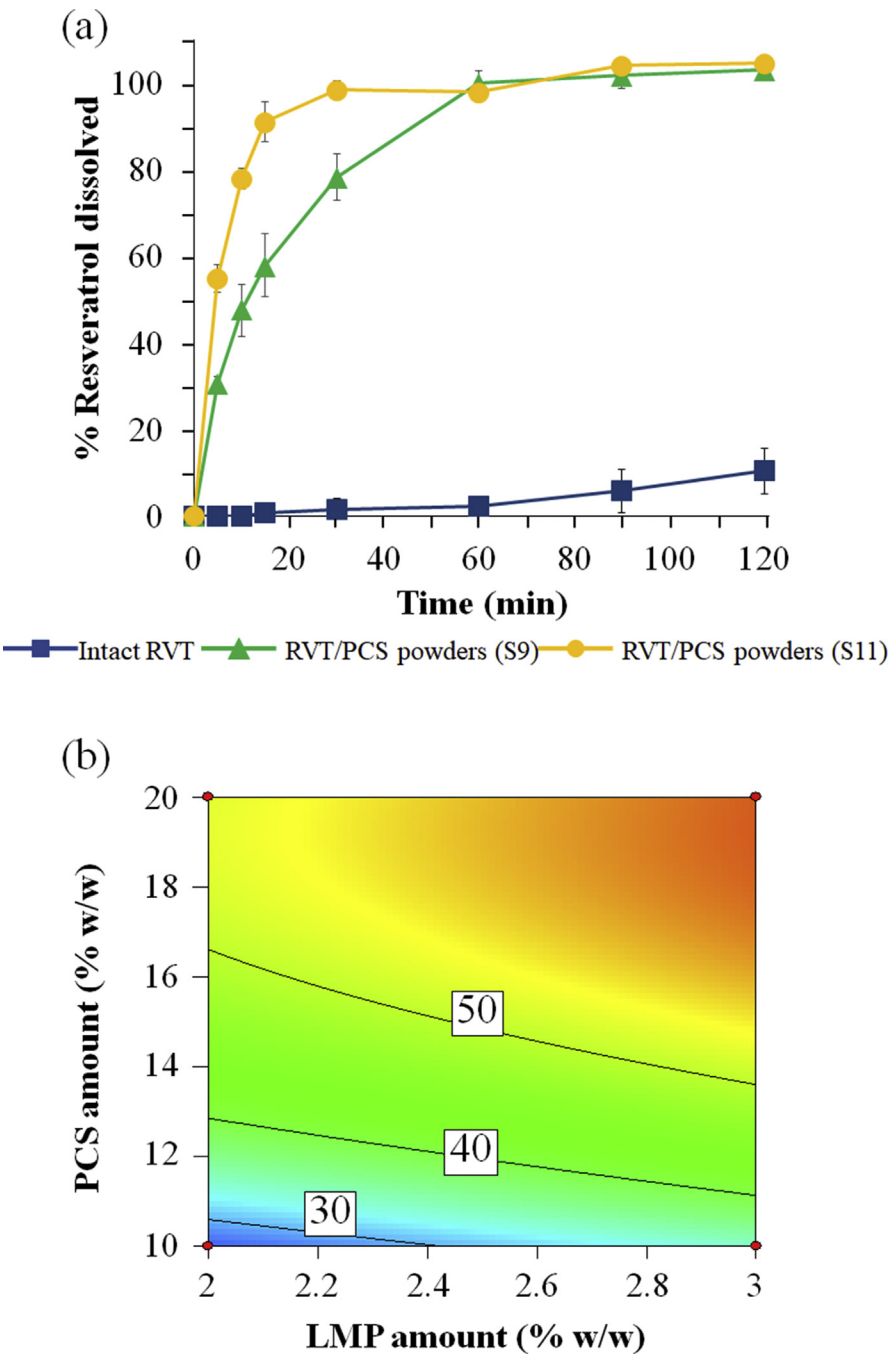

Fig. 5. (a) Dissolution profile of intact RVT and RVT/PCS powders (batch S9 and S11) and (b) contour plot showing the effect of PCS amount and low-methoxyl pectin (LMP) amount on drug dissolution at 5-min intervals in RVT/PCS powders.

only a few times larger than the size of an RVT single crystal. The formation of crystalline RVT after drying was restricted according to the limitation of the pore size of the PCS, which resulted in the reduction of the RVT crystal (to nano-sized) and an improvement in the dissolution properties of RVT. Other studies have reported that

https://doi.org/10.1016/j.heliyon.2019.e01399

the size reduction of poorly water-soluble drugs could be improved via adsorption onto porous powders [31, 33]. In addition, the physical state of RVT in the PCS was determined using PXRD measurement (Fig. 6a). From the PXRD patterns, intact RVT and physical mixture (PM) revealed sharp and highly intense diffraction

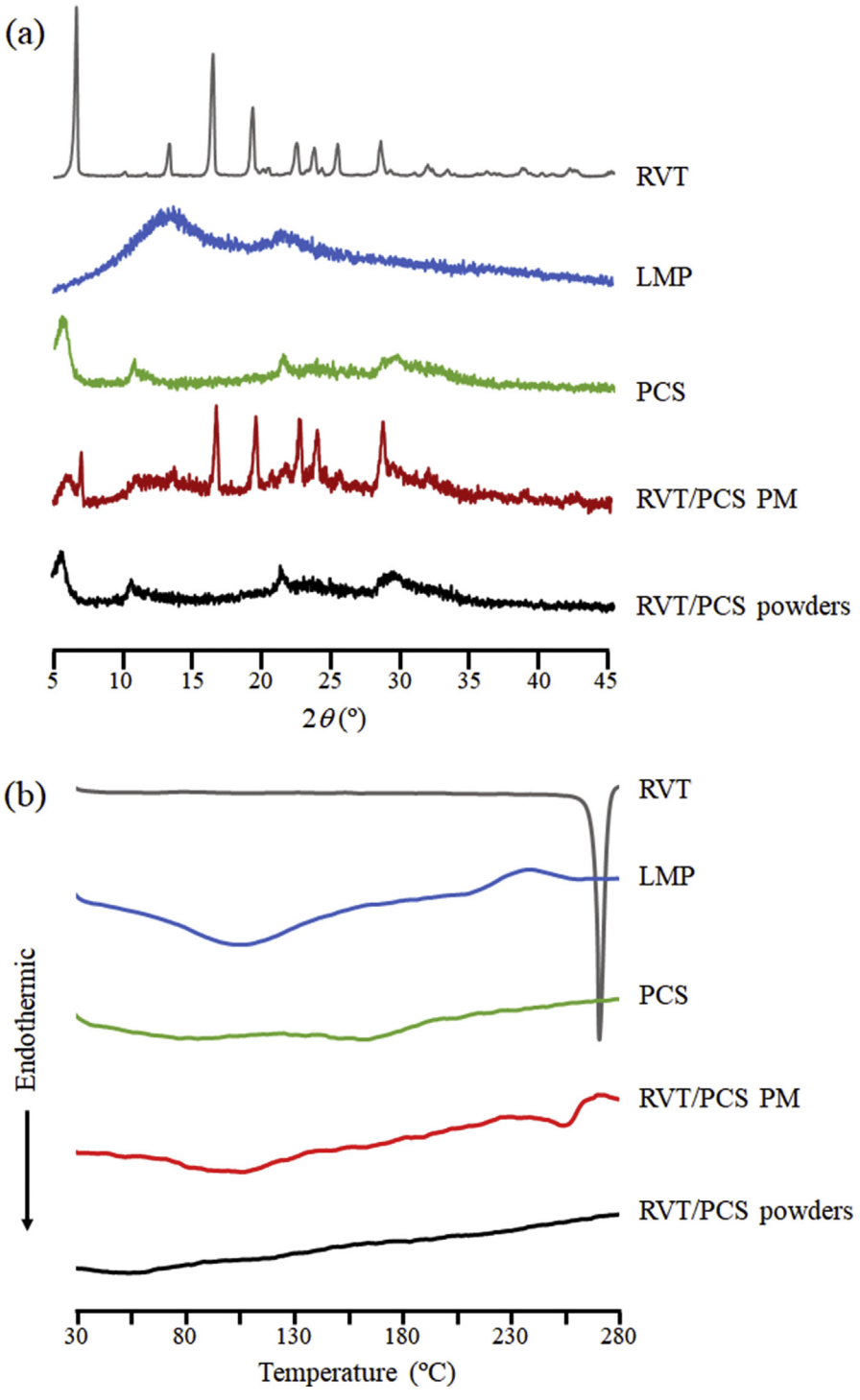

Fig. 6. (a) Powder X-ray patterns and (b) differential scanning calorimetry thermograms of RVT, LMP, PCS, RVT/PCS physical mixture (PM), and RVT/PCS powders.

https://doi.org/10.1016/j.heliyon.2019.e01399

peaks derived from crystal characteristics of RVT at 7°, 16°, 19°, 22°, 24°, and 28°. The PXRD pattern of RVT/PCS powders did not represent characteristic diffraction peaks of RVT crystal, indicating an absence of crystalline structure of RVT in the formulation. The thermal properties of RVT in the PCS powders were also evaluated by DSC (Fig. 6b). Intact RVT exhibited a melting endotherm at 270 °C, indicating its crystalline nature. The small melting endotherms of RVT presented in the PM but relative intensity peak was decreased. No obvious endothermic peak corresponding to the melting of crystalline RVT in the RVT/PCS powders, indicating that the drug was dispersed molecularly in the PCS [18].

The Q_5 of RVT/PCS powders varied from 21.48% ± 2.97%−63.54% ± 5.12% (Table 2). A mathematical model used to describe the relationship between the various factors and Q_5 of the RVT/PCS powders is shown in Eq. (9).

$$Q_5\,(\%):\ Y_3\ = +50.41\ +\ 3.67X_1\ +\ 12.49X_3 - 7.37X_3^2 \tag{9}$$

From the ANOVA results reported in Table 3, the mathematical model for predicting the Q_5 of RVT/PCS powders was significant (p-value < 0.0001) and lack of fit was not significant. A high r^2 value was also obtained for this model ($r^2 = 0.8014$). ANOVA showed that effect of PCS amount (X_3) and its quadratic term were the most significant. PCS amount showed a positive association with Q_5 of RVT/PCS powders. From the contour plot (Fig. 5b), an increase in PCS amount increased the dissolution properties of RVT when loaded onto the PCS powders. The RVT/PCS powders batch S11, which contained a higher amount of PCS, showed a relatively fast dissolution compared with batch S9 (Fig. 5a). The difference in Q_5 revealed that PCS amount affected the dissolution properties of RVT in RVT/PCS powders. During the mixing process, the RVT emulsion was dispersed and adsorbed onto the PCS surface. The high PCS amount resulted in a lower amount of RVT loaded onto the PCS powders, as discussed earlier, leading to an availability of free surface area on the PCS (i.e. with no drug adsorbed). An increase in free surface area may have yielded the fast dissolution of RVT. A large surface area could improve the dissolution properties of RVT/PCS powders [22, 34, 35].

3.4. Verification of mathematical model

The adequacy of the mathematical model was confirmed using three additional batches of RVT/PCS powders. Characterization for drug loading capacity, encapsulation efficiency and Q_5 were performed for these additional batches. The level of each factor, observed value (OV) and predicted value (PV) of the verification (V) batches are shown in Table 4. The RMSE was calculated to indicate the error of the model prediction [36]. The model of drug loading capacity response showed a low RMSE value, indicating that the model provided good predictability. However, the RMSE of the encapsulation and Q_5 prediction models was slightly higher than

https://doi.org/10.1016/j.heliyon.2019.e01399

Table 4. Verification experimental results for the model obtained from a Box−Behnken design of RVT/PCS powders.

Verification run (V)	Independent factors			Responses					
	LMP amount (% w/w)	EA amount (% w/w)	PCS amount (% w/w)	Drug loading capacity (%)		Encapsulation efficiency (%)		Q_5 (%)	
				OV	PV	OV	PV	OV	PV
V1	2.2	14	12	1.15 ± 0.01	1.13	85.59 ± 1.28	83.10	43.03 ± 8.04	38.06
V2	2.4	16	18	0.72 ± 0.04	0.85	72.51 ± 5.87	84.67	43.26 ± 0.75	54.52
V3	2.7	19	11	1.61 ± 0.03	1.80	83.52 ± 1.97	96.05	37.30 ± 4.45	37.17
RMSE					0.11		8.82		6.15

Q_5 = drug dissolution at 5-min intervals; OV = observed value; PV = predicted value.

that observed for the drug loading capacity model. Nevertheless, the results of each response obtained from each verification batch were found to be within 95% of the prediction interval of the PV (data not shown). Therefore, the models provided acceptable predictability and were suitable for prediction purposes.

3.5. Formulation optimization and characterization of optimized formulation

Once the responses were analyzed and the valid mathematical models were built, optimization was carried out to find the optimal range of the RVT/PCS formulations that provided satisfactory RVT/PCS powder quality. The criteria for each response of the RVT/PCS powders are shown in Table 5. The goal and limit of each response were specified based on the desired properties of the product. The drug loading capacity and encapsulation efficiency should be high to ensure a high amount of RVT in the RVT/PCS powders and a low amount of RVT loss during the manufacturing process. In addition, rapid drug dissolution is also preferred to provide rapid absorption of RVT in the gastrointestinal tract. Fig. 7 shows an established design space based on the criteria given in Table 5 being met. The optimized formulation could be produced with an LMP amount of 2.6% w/w. The amounts of EA and PCS used may be in the range shown in yellow in the design space (Fig. 7); however, the optimized formulation was produced using 19% w/w EA and 13% w/w PCS.

Table 5. Criteria of responses for formulation optimization of RVT/PCS powders.

Responses	Goal	Lower limit	Upper limit
Drug loading capacity (%)	maximize	1.5	2.2
Encapsulation efficiency (%)	maximize	80	100
Q_5 (%)	maximize	40	65

https://doi.org/10.1016/j.heliyon.2019.e01399

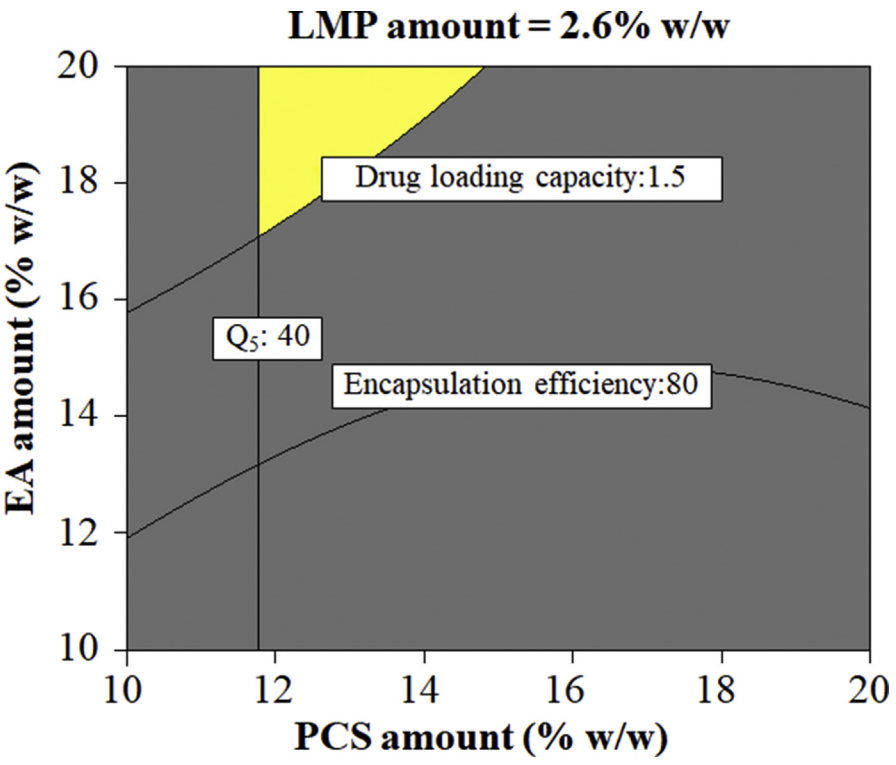

Fig. 7. Overall design space to satisfy the criteria for all responses of the RVT/PCS powders in Table 5. The design space is represented by the yellow area.

The results for the optimized RVT/PCS powders are shown in Table 6. The optimized formulation showed a high drug loading capacity of 1.55% ± 0.01%. The encapsulation efficiency of the optimized formulation was 93.76% ± 1.08%, indicating the high amount of RVT encapsulated in the porous powders. The Q_5 of the optimized RVT/PCS powders was 43.55% ± 2.24%. The dissolution profile of the optimized formulation, as compared with intact RVT, is presented in Fig. 8a. The dissolution properties of RVT in the optimized formulation were enhanced compared with intact RVT, as was observed in the Box−Behnken design experimental results. The response results of the optimized formulation were close to the PVs, with a small percent error (<4%); this confirms the validity of the prediction models (Table 6). The optimized RVT/PCS powders were further evaluated for bulk density. LMP is a polymeric surfactant and is used to improve the bulk density of PCS powders. The bulk density of the intact PCS powders was 0.061 ± 0.001 g/cm^3. The PCS powders containing the same amount of RVT but without LMP showed similar bulk densities to those of intact PCS, i.e. 0.065 ± 0.003 g/cm3, whereas the bulk densities of the optimized RVT/PCS powders showed a 70% increase, i.e. 0.102 ± 0.016 g/cm^3. The addition of LMP to the formulation increased the bulk density of PCS in the RVT/PCS powders. This increase facilitates certain manipulations during the manufacturing process, especially in relation to solid formulation.

https://doi.org/10.1016/j.heliyon.2019.e01399

Table 6. Experimental results of the optimized RVT/PCS powder formulation.

Responses	Observed value	Predicted value	Residual	Error (%)
Drug loading capacity (%)	1.55 ± 0.02	1.59	1.44	2.66
Encapsulation efficiency (%)	93.76 ± 1.08	92.24	-1.52	1.65
Q_5 (%)	43.55 ± 2.24	44.97	1.42	3.16

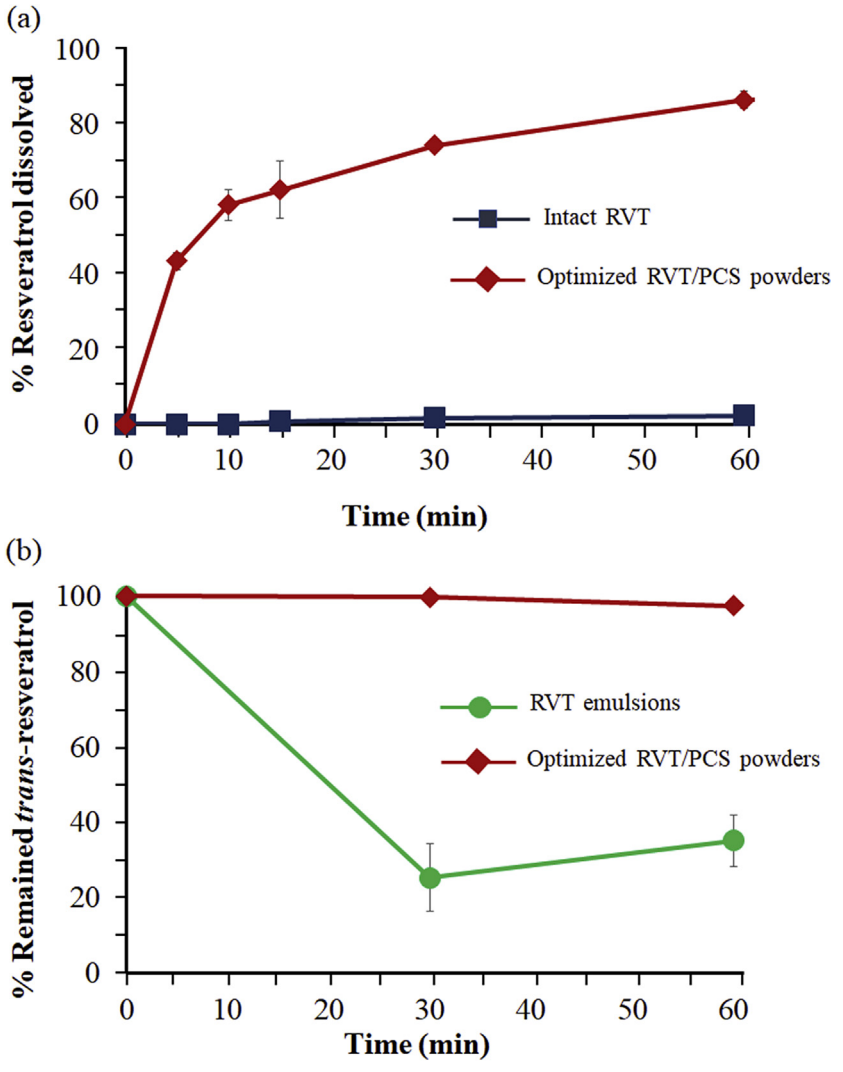

Fig. 8. (a) Dissolution profile of intact RVT and optimized RVT/PCS powders and (b) remaining *trans*-RVT after UV exposure of RVT emulsions and optimized RVT/PCS powders.

3.6. Photostability of RVT in optimized RVT/PCS powders

The photostability of RVT in the optimized RVT/PCS powders and RVT emulsions consisted of the same amount of RVT in the optimized RVT/PCS powders

https://doi.org/10.1016/j.heliyon.2019.e01399

is shown in Fig. 8b. The *trans*-RVT isomer was transformed via UV irradiation to the cis-RVT isomer [37]. RVT, in the *trans*-isomer, in RVT emulsions was degraded rapidly and only 25.34% ± 8.90% and 35.14% ± 6.94% of the *trans*-RVT remained after UV irradiation for 30 min and 60 min, respectively as shown in Fig 8b. Remained *trans*-RVT in RVT emulsions exhibited slightly higher photostability than that in RVT in ethanolic solution (data not shown). This is probably due to the fact that RVT was encapsulated in the emulsions. The optimized formulation showed remaining *trans*-RVT of 94.61% ± 3.46% and 97.48% ± 3.78% after UV irradiation for 30 min and 60 min, respectively. RVT could be effectively protected from UV irradiation when loaded onto the porous powders. Previous studies have reported that the stability of RVT is enhanced using techniques such as polymer matrix and acrylate microspheres [10, 38, 39]. However, some chemical degradation of *trans*-RVT was observed after 60-min UV exposure. In this experiment, the relatively high amount of *trans*-RVT still remaining after UV irradiation for 60 min indicates the effectiveness of the PCS powders in protecting the UV-sensitive compound.

4. Conclusions

The present study demonstrates that the dissolution properties of RVT were improved by RVT/PCS powder formulation. The effect of three independent factors, LMP amount, EA amount and PCS amount, on drug loading capacity, encapsulation efficiency and Q_5 were studied using the Box−Behnken design. The experimental results showed that EA amount and PCS amount had significant effects on the drug loading capacity. The encapsulation efficiency was significantly influenced by EA amount. The PCS amount had a significant effect on Q_5. The optimized RVT/PCS formulation showed that drug loading capacity, encapsulation efficiency and Q_5 met all the satisfying criteria. Based on the dissolution profile, fast dissolution of RVT was obtained within 5-min intervals. In addition, the bulk density of PCS was improved by the addition of LMP to the formulation and RVT/PCS powder formulation could protect RVT from UV irradiation, resulting in the chemical stability of RVT in PCS powders. The development of RVT products using PCS powders could improve their dissolution properties, their stability after UV irradiation of RVT and the bulk density of PCS powders. Furthermore, the experimental design and optimization technique could be applied to the development of pharmaceutical products; thus providing an extensive understanding of the relationship between formulation and product quality. Even though this study that the photostability of RVT was improved, however, the thermal stability improvement of RVT in the PCS should be studied in the future.

https://doi.org/10.1016/j.heliyon.2019.e01399

Declarations

Author contribution statement

Pontip Benjasirimongkol: Performed the experiments; Analyzed and interpreted the data; Wrote the paper.

Suchada Piriyaprasarth: Conceived and designed the experiments; Analyzed and interpreted the data; Contributed reagents, materials, analysis tools or data.

Pornsak Sriamornsak: Conceived and designed the experiments; Analyzed and interpreted the data; Wrote the paper.

Funding statement

This research did not receive any specific grant from funding agencies in the public, commercial, or not-for-profit sectors.

Competing interest statement

The authors declare no conflict of interest.

Additional information

No additional information is available for this paper.

Acknowledgements

The authors would like to thank Eisai R&D Management Co., Ltd. for providing Florite® RE sample.

References

[1] A. Tresserra-Rimbau, R.M. Lamuela-Raventos, J.J. Moreno, Polyphenols, food and pharma. Current knowledge and directions for future research, Biochem. Pharmacol. (2018) 186−195.

[2] G. Williamson, C.D. Kay, A. Crozier, The bioavailability, transport, and bioactivity of dietary flavonoids: a review from a historical perspective, Compr. Rev. Food Sci. Food Saf. (2018) 1054−1112.

[3] F. Perez-Vizcaino, C.G. Fraga, Research trends in flavonoids and health, Arch. Biochem. Biophys. 646 (2018) 107−112.

[4] N.K.R. Ghattamaneni, S.K. Panchal, L. Brown, Nutraceuticals in rodent models as potential treatments for human inflammatory bowel disease, Pharmacol. Res. 132 (2018) 99−107.

https://doi.org/10.1016/j.heliyon.2019.e01399

[5] A.B. Santhakumar, M. Battino, J.M. Alvarez-Suarez, Dietary polyphenols: structures, bioavailability and protective effects against atherosclerosis, Food Chem. Toxicol. 113 (2018) 49–65.

[6] M.G. Novelle, D. Wahl, C. Diéguez, M. Bernier, R. de Cabo, Resveratrol supplementation: where are we now and where should we go? Ageing Res. Rev. 21 (2015) 1–15.

[7] K.E. Allan, C.E. Lenehan, A.V. Ellis, UV light stability of α-cyclodextrin/resveratrol host–guest complexes and isomer stability at varying pH, Aust. J. Chem. 62 (2009) 921–926.

[8] Z.-L. Wan, J.-M. Wang, L.-Y. Wang, X.-Q. Yang, Y. Yuan, Enhanced physical and oxidative stabilities of soy protein-based emulsions by incorporation of a water-soluble stevioside–resveratrol complex, J. Agric. Food Chem. 61 (2013) 4433–4440.

[9] P. Benjasirimongkol, P. Sriamornsak, Stability study of resveratrol-loaded emulsions using pectin as an emulsifier, Asian J. Pharm. Sci. 11 (2016) 199–200.

[10] F. Liu, D. Ma, X. Luo, Z. Zhang, L. He, Y. Gao, D.J. McClements, Fabrication and characterization of protein-phenolic conjugate nanoparticles for co-delivery of curcumin and resveratrol, Food Hydrocoll. 79 (2018) 450–461.

[11] Y. Zu, H. Overby, G. Ren, Z. Fan, L. Zhao, S. Wang, Resveratrol liposomes and lipid nanocarriers: comparison of characteristics and inducing browning of white adipocytes, Colloids Surfaces B Biointerfaces 164 (2018) 414–423.

[12] J.G. Cheng, B.R. Tian, Q. Huang, H.R. Ge, Z.Z. Wang, Resveratrol functionalized carboxymethyl-β-cyclodextrin: synthesis, characterization, and photostability, J. Chem. (2018), 6789076.

[13] C.B. Detoni, G.D. Souto, A.L.M. da Silva, A.R. Pohlmann, S.S. Guterres, Photostability and skin penetration of different *E*-resveratrol-loaded supramolecular structures, Photochem. Photobiol. 88 (2012) 913–921.

[14] I.J. Joye, G. Davidov-Pardo, D.J. McClements, Encapsulation of resveratrol in biopolymer particles produced using liquid antisolvent precipitation. Part 2: stability and functionality, Food Hydrocoll 49 (2015) 127–134.

[15] J. Chen, N. Wei, M. Lopez-Garcia, D. Ambrose, J. Lee, C. Annelin, T. Peterson, Development and evaluation of resveratrol, vitamin E, and epigallocatechin gallate loaded lipid nanoparticles for skin care applications, Eur. J. Pharm. Biopharm. 117 (2017) 286–291.

https://doi.org/10.1016/j.heliyon.2019.e01399

[16] I. Yasuyuki, S. Uchida, N. Namiki, Preparation and evaluation of orally disintegrating tablets containing vitamin E as a model fat-soluble drug, Chem. Pharm. Bull. 63 (2015) 156−163.

[17] Y. Weerapol, S. Limmatvapirat, H. Takeuchi, P. Sriamornsak, Fabrication of spontaneous emulsifying powders for improved dissolution of poorly water-soluble drugs, Powder Technol. 271 (2015) 100−108.

[18] Y. Weerapol, S. Limmatvapirat, C. Jansakul, H. Takeuchi, P. Sriamornsak, Enhanced dissolution and oral bioavailability of nifedipine by spontaneous emulsifying powders: effect of solid carriers and dietary state, Eur. J. Pharm. Biopharm. 91 (2015) 25−34.

[19] M. Zhou, L. Shen, X. Lin, Y. Hong, Y. Feng, Design and pharmaceutical applications of porous particles, RSC Adv. 7 (2017) 39490−39501.

[20] Y. Fujimoto, N. Hirai, T. Takatani-Nakase, K. Takahashi, Novel tablet formulation of amorphous indomethacin using wet granulation with a high-speed mixer granulator combined with porous calcium silicate, J. Drug Deliv. Sci. Technol. 33 (2016) 51−57.

[21] S. Piriyaprasarth, P. Sriamornsak, Effect of source variation on drug release from HPMC tablets: linear regression modeling for prediction of drug release, Int. J. Pharm. 411 (2011) 36−42.

[22] S. Sharma, A. Pawar, Low density multiparticulate system for pulsatile release of meloxicam, Int. J. Pharm. 313 (2006) 150−158.

[23] M. Ghasemnejad, E. Ahmadi, Z. Mohamadnia, A. Doustgani, S. Hashemikia, Functionalized silica nanoparticles as a carrier for Betamethasone Sodium Phosphate: drug release study and statistical optimization of drug loading by response surface method, Mater. Sci. Eng. C 56 (2015) 223−232.

[24] ICH (International Conference on Harmonization), Pharmaceutical Development, Q8R2, 2009. Accessed November 2016, http://www.ich.org/fileadmin/Public_Web_Site/ICH_Products/Guidelines/Quality/Q8_R1/Step4/Q8_R2_Guideline.pdf.

[25] C.J. Willmott, Some comments on the evaluation of model performance, Bull. Am. Meteorol. Soc. 63 (1982) 1309−1313.

[26] K. Burapapadh, H. Takeuchi, P. Sriamornsak, Development of pectin nanoparticles through mechanical homogenization for dissolution enhancement of itraconazole, Asian J. Pharm. Sci. 11 (2016) 365−375.

https://doi.org/10.1016/j.heliyon.2019.e01399

[27] P. Sher, G. Ingavle, S. Ponrathnam, A.P. Pawar, Low density porous carrier: drug adsorption and release study by response surface methodology using different solvents, Int. J. Pharm. 331 (2007) 72−83.

[28] P. Sher, G. Ingavle, S. Ponrathnam, A.P. Pawar, Low density porous carrier based conceptual drug delivery system, Microporous Mesoporous Mater. 102 (2007) 290−298.

[29] R.M. Pires, H.F. Costa, A.G.M. Ferreira, I.M.A. Fonseca, Viscosity and density of water + ethyl acetate + ethanol mixtures at 298.15 and 318.15 K and atmospheric pressure, J. Chem. Eng. Data 52 (2007) 1240−1245.

[30] P.F. Germann, L. DiPietro, When is porous-media flow preferential? A hydromechanical perspective, Geoderma 74 (1996) 1−21.

[31] M.T. Ali, R. Fule, A. Sav, P. Amin, Porous starch: a novel carrier for solubility enhancement of carbamazepine, AAPS Pharm. Sci. Tech. 14 (2013) 919−926.

[32] F. Caruso, J. Tanski, A. Villegas-Estrada, M. Rossi, Structural basis for antioxidant activity of *trans*-resveratrol: Ab Initio calculations and crystal and molecular structure, J. Agric. Food Chem. 52 (2004) 7279−7285.

[33] A. Godec, U. Maver, M. Bele, O. Planinšek, S. Srčič, M. Gaberšček, J. Jamnik, Vitrification from solution in restricted space: formation and stabilization of amorphous nifedipine in a nanoporous silica xerogel carrier, Int. J. Pharm. 343 (2007) 131−140.

[34] R. Mellaerts, C.A. Aerts, J. Van Humbeeck, P. Augustijns, G. Van den Mooter, J.A. Martens, Enhanced release of itraconazole from ordered mesoporous SBA-15 silica materials, Chem. Commun. (2007) 1375−1377.

[35] C. Faruk, Scale effect on porosity and permeability: kinetics, model, and correlation, AIChE J. 47 (2001) 271−287.

[36] T. Chai, R. Draxler, Root mean square error (RMSE) or mean absolute error (MAE)? − Arguments against avoiding RMSE in the literature, Geosci. Model Dev. (2014) 1247−1250, 2014.

[37] C.G. Silva, J. Monteiro, R.R. Marques, A.M. Silva, C. Martínez, M. Canle, J.L. Fariaa, Photochemical and photocatalytic degradation of *trans*-resveratrol, Photochem. Photobiol. Sci. 12 (2013) 638−644.

[38] R. Pignatello, T.M.G. Pecora, G.G. Cutuli, A. Catalfo, G. De Guidi, B. Ruozi, G. Tosi, S. Cianciolo, T. Musumeci, Antioxidant activity and photostability assessment of *trans*-resveratrol acrylate microspheres, Pharmaceut. Dev. Technol. 24 (2) (2019) 222−234.

https://doi.org/10.1016/j.heliyon.2019.e01399

[39] C.C. Koga, J.E. Andrade, M.G. Ferruzzi, Y. Lee, Stability of *trans*-resveratrol encapsulated in a protein matrix produced using spray drying to UV light stress and simulated gastro-intestinal digestion, J. Food Sci. 81 (2015) C292–C300.

https://doi.org/10.1016/j.heliyon.2019.e01399